



**AFRL-RX-WP-JA-2015-0143**

**SYNTHESIS AND REACTIVITY OF ALUMINIZED  
FLUORINATED ACRYLIC (AIFA) NANOCOMPOSITES  
(POSTPRINT)**

**Christian J. Pierce and Jonathan E. Spowart  
AFRL/RXCM**

**Christopher A. Crouse  
UES, Inc.**

**APRIL 2014  
Interim Report**

**Distribution Statement A. Approved for public release; distribution unlimited.**

*See additional restrictions described on inside pages*

**STINFO COPY**

**© 2012 Published by Elsevier Inc. on behalf of The Combustion Institute**

**AIR FORCE RESEARCH LABORATORY  
MATERIALS AND MANUFACTURING DIRECTORATE  
WRIGHT-PATTERSON AIR FORCE BASE OH 45433-7750  
AIR FORCE MATERIEL COMMAND  
UNITED STATES AIR FORCE**

## NOTICE AND SIGNATURE PAGE

Using Government drawings, specifications, or other data included in this document for any purpose other than Government procurement does not in any way obligate the U.S. Government. The fact that the Government formulated or supplied the drawings, specifications, or other data does not license the holder or any other person or corporation; or convey any rights or permission to manufacture, use, or sell any patented invention that may relate to them.

Qualified requestors may obtain copies of this report from the Defense Technical Information Center (DTIC) (<http://www.dtic.mil>).

AFRL-RX-WP-JA-2015-0143 HAS BEEN REVIEWED AND IS APPROVED FOR PUBLICATION IN ACCORDANCE WITH ASSIGNED DISTRIBUTION STATEMENT.

//Signature//

---

MICHEAL E. BURBA, Project Engineer  
Metals Branch  
Structural Materials Division

//Signature//

---

DANIEL J. EVANS, Chief  
Metals Branch  
Structural Materials Division

//Signature//

---

ROBERT T. MARSHALL, Deputy Chief  
Structural Materials Division  
Materials And Manufacturing Directorate

This report is published in the interest of scientific and technical information exchange and its publication does not constitute the Government's approval or disapproval of its ideas or findings.

# REPORT DOCUMENTATION PAGE

Form Approved  
OMB No. 0704-0188

The public reporting burden for this collection of information is estimated to average 1 hour per response, including the time for reviewing instructions, searching existing data sources, gathering and maintaining the data needed, and completing and reviewing the collection of information. Send comments regarding this burden estimate or any other aspect of this collection of information, including suggestions for reducing this burden, to Department of Defense, Washington Headquarters Services, Directorate for Information Operations and Reports (0704-0188), 1215 Jefferson Davis Highway, Suite 1204, Arlington, VA 22202-4302. Respondents should be aware that notwithstanding any other provision of law, no person shall be subject to any penalty for failing to comply with a collection of information if it does not display a currently valid OMB control number. **PLEASE DO NOT RETURN YOUR FORM TO THE ABOVE ADDRESS.**

<b>1. REPORT DATE (DD-MM-YY)</b> April 2014		<b>2. REPORT TYPE</b> Interim		<b>3. DATES COVERED (From - To)</b> 19 March 2014 – 31 March 2014	
<b>4. TITLE AND SUBTITLE</b> SYNTHESIS AND REACTIVITY OF ALUMINIZED FLUORINATED ACRYLIC (ALFA) NANOCOMPOSITES (POSTPRINT)				<b>5a. CONTRACT NUMBER</b> In-house	
				<b>5b. GRANT NUMBER</b>	
				<b>5c. PROGRAM ELEMENT NUMBER</b> 62102F	
<b>6. AUTHOR(S)</b> Christian J. Pierce and Jonathan E. Spowart - AFRL/RXCM Christopher A. Crouse - UES, Inc.				<b>5d. PROJECT NUMBER</b> 4349	
				<b>5e. TASK NUMBER</b>	
				<b>5f. WORK UNIT NUMBER</b> X0W6	
<b>7. PERFORMING ORGANIZATION NAME(S) AND ADDRESS(ES)</b>  AFRL/RXCM 2941 Hobson Way Bldg 654, Rm 136 Wright-Patterson AFB, OH 45433				<b>8. PERFORMING ORGANIZATION REPORT NUMBER</b>	
<b>9. SPONSORING/MONITORING AGENCY NAME(S) AND ADDRESS(ES)</b>  Air Force Research Laboratory Materials and Manufacturing Directorate Wright-Patterson Air Force Base, OH 45433-7750 Air Force Materiel Command United States Air Force				<b>10. SPONSORING/MONITORING AGENCY ACRONYM(S)</b> AFRL/RXCM	
				<b>11. SPONSORING/MONITORING AGENCY REPORT NUMBER(S)</b> AFRL-RX-WP-JA-2015-0143	
<b>12. DISTRIBUTION/AVAILABILITY STATEMENT</b> Distribution Statement A. Approved for public release; distribution unlimited.					
<b>13. SUPPLEMENTARY NOTES</b> Journal article published in <i>Combustion and Flame</i> 159 (2012) 3199-3207. ©2012 Published by Elsevier Inc. on behalf of The Combustion Institute. The U.S. Government is joint author of the work and has the right to use, modify, reproduce, release, perform, display or disclose the work. This report contains color. The final publication is available at <a href="http://dx.doi.org/10.1016/j.combustflame.2012.03.016">http://dx.doi.org/10.1016/j.combustflame.2012.03.016</a> .					
<b>14. ABSTRACT</b> Fluorinated materials, such as poly(tetrafluoroethylene) and its co-polymers, have attracted significant interest throughout the energetic materials community due to their strong reactivity with aluminum powders. Herein, we report the synthesis of a novel composite material produced through the <i>in situ</i> polymerization of 1H,1H,2H,2H-perfluorodecyl methacrylate in the presence of aluminum nanoparticles which have been previously functionalized with phosphoric acid 2-hydroxyethyl methacrylate ester to promote chemical integration into the polymer matrix. These materials, which we have termed aluminized fluorinated acrylic (AIFA) composites, have been prepared with particle contents ranging from 10% to 70% by weight. At particle loadings of 60 wt.% or less, the AIFA composites exhibited thermoplastic behavior and were able to be processed by melt extrusion. The AIFA-50 composite demonstrated the highest reactivity (most intense flame and shortest time to achieve complete deflagration) during air combustion experiments performed on consolidated pellets. Chemical analysis of the char indicated the presence of AlF <sub>3</sub> , in addition to Al <sub>2</sub> O <sub>3</sub> , Al <sub>4</sub> C <sub>3</sub> and residual Al, indicating that reaction with the fluoropolymer matrix does result in fluorination of the aluminum during the deflagration, however, this mechanism competes kinetically with air oxidation and carbide formation at higher particle loadings.					
<b>15. SUBJECT TERMS</b> aluminum, aluminum nanoparticles, fluoropolymer, reactive composites					
<b>16. SECURITY CLASSIFICATION OF:</b>			<b>17. LIMITATION OF ABSTRACT:</b>  SAR	<b>18. NUMBER OF PAGES</b>  12	<b>19a. NAME OF RESPONSIBLE PERSON (Monitor)</b> Micheal E. Burba <b>19b. TELEPHONE NUMBER (Include Area Code)</b> (937) 255-9795
<b>a. REPORT</b> Unclassified	<b>b. ABSTRACT</b> Unclassified	<b>c. THIS PAGE</b> Unclassified			



# Synthesis and reactivity of aluminized fluorinated acrylic (AIFA) nanocomposites

Christopher A. Crouse<sup>a,b,\*</sup>, Christian J. Pierce<sup>a</sup>, Jonathan E. Spowart<sup>a</sup>

<sup>a</sup> Air Force Research Laboratory, Materials and Manufacturing Directorate, Wright-Patterson Air Force Base, OH 45433, United States

<sup>b</sup> UES, Inc., Dayton, OH 45432, United States

## ARTICLE INFO

### Article history:

Received 17 November 2011

Received in revised form 14 March 2012

Accepted 23 March 2012

Available online 18 June 2012

### Keywords:

Aluminum

Aluminum nanoparticles

Fluoropolymer

Reactive composites

## ABSTRACT

Fluorinated materials, such as poly(tetrafluoroethylene) and its co polymers, have attracted significant interest throughout the energetic materials community due to their strong reactivity with aluminum powders. Herein, we report the synthesis of a novel composite material produced through the *in situ* polymerization of 1H,1H,2H,2H perfluorodecyl methacrylate in the presence of aluminum nanoparticles which have been previously functionalized with phosphoric acid 2 hydroxyethyl methacrylate ester to promote chemical integration into the polymer matrix. These materials, which we have termed aluminized fluorinated acrylic (AIFA) composites, have been prepared with particle contents ranging from 10% to 70% by weight. At particle loadings of 60 wt.% or less, the AIFA composites exhibited thermoplastic behavior and were able to be processed by melt extrusion. The AIFA 50 composite demonstrated the highest reactivity (most intense flame and shortest time to achieve complete deflagration) during air combustion experiments performed on consolidated pellets. Chemical analysis of the char indicated the presence of  $AlF_3$ , in addition to  $Al_2O_3$ ,  $Al_4C_3$  and residual Al, indicating that reaction with the fluoro polymer matrix does result in fluorination of the aluminum during the deflagration, however, this mechanism competes kinetically with air oxidation and carbide formation at higher particle loadings.

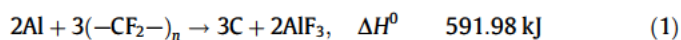
© 2012 Published by Elsevier Inc. on behalf of The Combustion Institute.

## 1. Introduction

Aluminum powders are a critical ingredient in the formulation of many energetic materials, including some explosives and propellants, added to increase energy densities within these systems as well as enhance their flame temperatures and pressures [1]. Micron scale aluminum (micron Al) powders are used in nearly all conventional metalized energetic materials, however, the advent of technologies to produce high quality nano scale aluminum powders (nano Al) has led to the exploration of nano Al as a replacement for micron Al in certain formulations [2,3]. The interest in nano Al as a replacement for larger micron Al powders stems from the dramatic increase in specific surface area (SSA) that is obtained as a result of the small particle size of the nano powders. The large SSA, typically 25–40 m<sup>2</sup>/g, yields an increase in the reactive performance of these materials due to the close proximity of the fuel (nano Al) and oxidizing components of these systems, as the kinetics for these reactions are generally limited by mass transport (diffusion) between the reacting species [1,4]. For example, substitution of nano Al for micron Al in a thermite mixture, e.g., aluminum powder mixed with a metastable metal oxide

( $Fe_2O_3$ , CuO,  $Bi_2O_3$ ,  $WO_3$ , etc.), can lead to an increase in the rate of reaction by up to three orders of magnitude [5,6].

Fluorinated materials, specifically fluorinated polymers such as poly(tetrafluoroethylene) (PTFE) and its co polymers, fluorinated elastomers, and molecular fluorocarbons have recently received significant attention as suitable oxidizer materials for nano Al [7–9]. The stoichiometric reaction of Al with a pure fluorocarbon (e.g., PTFE;  $\Delta H_F = 809.60$  kJ/mol) [10] yields elemental carbon and aluminum trifluoride as shown in the following equation:



Formation of  $AlF_3$  ( $\Delta H_F(AlF_3) = 1510.39$  kJ/mol) yields 56.10 kJ/g of Al which is nearly twice the energy liberated by reacting Al with oxygen to yield  $Al_2O_3$  ( $\Delta H_F(Al_2O_3) = 1675.72$  kJ/mol), which results in 30.98 kJ/g of Al [11]. Additionally,  $AlF_3$  begins to sublime at 1276 °C well below the combustion temperature of nano Al [11]. As  $AlF_3$  volatilizes it should leave behind a fresh aluminum surface which can enhance the kinetics of the reaction as there is less build up of product on the particle surface to inhibit diffusion between the reactants. This is contrary to aluminum oxidation where the combustion temperature is limited to an extent by the vaporization temperature of the oxide ( $T_{vap} = ca. 3000–3700$  °C) as more oxide is formed the reaction rate can actually begin to slow down due to the presence of the dense molten alumina at the surface of the particle, since the boiling temperature of aluminum is less than the vaporization temperature of the oxide the aluminum

\* Corresponding author at: Air Force Research Laboratory, Materials and Manufacturing Directorate, Wright-Patterson Air Force Base, OH 45433, United States.

E-mail address: [christopher.crouse.ctr@wpafb.af.mil](mailto:christopher.crouse.ctr@wpafb.af.mil) (C.A. Crouse).

fuel must diffuse through the oxide to react with oxygen in the vapor phase [11,12]. The potential increase in liberated energy and energy release rate makes fluorinated materials viable alternatives to conventional metal oxide powders in several applications.

Reactive mixtures where the fuel and oxidizer components are both powders (e.g., Al and Fe<sub>2</sub>O<sub>3</sub>) are typically consolidated by powder compaction. This often results in a material that is brittle due to an absence of chemical bonding and/or strong physical interaction between the individual particles. The mechanical properties of pressed powder composites can be improved by the addition of a binder material, however, these materials are often inert and subtract from the performance of the material [13]. Additionally, due to the high SSA of the nano powders, a significant amount of binder is required to provide complete coverage of the powders. The addition of fluorinated polymers, or reactive polymers in general, as either an oxidizer or reactive binder has the potential to introduce useful mechanical properties into these reactive powder mixtures. Reactive mixtures of nano Al with PTFE or PTFE/Viton represents current state of the art for reactive nano Al/fluoropolymer systems [7,8,14]. In most literature reports these composites are prepared by sonochemical mixing of nano Al with PTFE or PTFE/Viton powders in a solvent to evenly distribute and increase contact between the components. Consolidation of the mixtures is achieved by evaporation of the solvent and compression of the mixed powders into pellet form [7,15]. Fluoropolymers are soft in comparison to nano Al and the composites can often be pressed to near uniform density without undergoing any elevated temperature processing or sintering. However, the consolidated pressed powder composites have minimal chemical and/or physical interaction between the individual component particles (polymer + metal and polymer + polymer), and thereby fail to achieve adequate mechanical properties. To obtain better bonding between the individual components, additional processing steps such as sintering or extrusion can be performed, however, sintering of PTFE is typically performed at temperatures above 300–400 °C which is near the temperature required to initiate pre ignition reactions; i.e. reactions with the amorphous aluminum oxide shell on nano Al [9]. Processing of PTFE by extrusion is also not possible without addition of other chemicals and/or solvents or modification of the polymer backbone to yield a co polymer [16].

Herein we report a new approach towards the preparation of nano Al/fluoropolymer composites, comprised of functionalized nano Al chemically integrated into a fluorinated methacrylic polymer through an *in situ* polymerization process. These aluminized fluorinated acrylic nanocomposites, which we have termed AIFA composites, show good bonding at the polymer and particle interface and exhibit thermoplastic behavior allowing them to be processed using conventional polymer processing techniques such as melt extrusion. A detailed description of the synthetic approach and characterization of their physical properties and reactive behavior is discussed.

## 2. Experimental

### 2.1. Chemicals

Aluminum nanoparticles (80 nm, 80% active Al content) were obtained from Novacentrix, Inc. and were stored under argon in a glove box (O<sub>2</sub> ≤ 1 ppm; dew point = 80 °C) prior to use. Cyclohexanone, phosphoric acid 2 hydroxyethyl methacrylate ester (PAM) and 2,2' azobis(2 methylpropionitrile) (AIBN) were acquired from Aldrich and used as received unless otherwise noted. 1H,1H,2H,2H perfluorodecyl methacrylate (PFDMA) was obtained from Synquest Laboratories and purified by vacuum distillation and stored under nitrogen in a refrigerator (4 °C) prior to use.

Cyclohexanone was dried over CaH<sub>2</sub> and distilled prior to use in the polymerizations. AIBN was recrystallized from acetone prior to use.

### 2.2. Synthesis of PAM co nano Al

The procedure used for the surface functionalization of nano Al with PAM prior to composite formation was adapted from previous literature [17]. A typical reaction for the functionalization of nano Al with PAM to yield PAM co nano Al was performed as follows. A 1000 mL four necked reaction vessel, fitted with an overhead stirrer, two rubber septa, and a glass stopper was charged with nano Al powder (30.0 g, 1.11 mol) and hydroquinone (0.050 g, 0.45 mmol), which was added as a radical scavenger to prevent polymerization during the reaction. PAM (2.97 g, 12.5 mmol) [18] was dissolved into 250 mL of cyclohexanone and transferred to the reaction vessel and stirred (235 rpm). A nitrogen atmosphere was established and maintained in the reaction vessel throughout the course of reaction. The vessel was then submerged into an external oil bath at 60 °C and reaction was allowed to progress for 4 h. The functionalized particles were isolated by vacuum filtration over a 0.2 μm PTFE membrane (Cole Parmer) and washed with cyclohexanone and acetone to remove physisorbed PAM. The filtered product was then dried in a vacuum desiccator to remove residual solvent prior to analysis. Organic content of the PAM co nano Al was determined to be ca. 4% by weight.

### 2.3. Synthesis of aluminized fluorinated acrylic (AIFA) composites

AIFA X (where X denotes the particle content in terms of particle wt.%) composites were prepared by *in situ* polymerization of PFDMA with varying concentrations of PAM co nano Al as indicated in Table 1. A typical polymerization for the preparation of AIFA 30 was carried out using the following procedure. A 1000 mL four necked reaction vessel fitted with an overhead stirrer and three rubber septa was charged with PAM co nano Al (15.0 g) and AIBN (0.350 g, 2.13 mmol). The vessel was then sealed and placed under a nitrogen atmosphere. PFDMA (35.0 g, 65.8 mmol) was added via syringe to the reaction vessel followed by dry cyclohexanone (75 mL) which was transferred via canula to serve as the solvent. The reaction mixture was subjected to three purge freeze pump thaw cycles to remove dissolved oxygen. Upon completion the mixture was stirred at 235 rpm and the reaction vessel was submerged into an external oil bath held at 75 °C for a minimum of 4 h. In most cases polymerization was completed prior to 4 h and could be observed by an increase in viscosity and precipitation of the composite from the solvent, however, the reaction was still held at temperature for 4 h to ensure the complete polymerization. After 4 h the heat was removed and the reaction was allowed to cool to room temperature. The composite was removed from the reaction vessel, transferred to a filtration apparatus fitted with a 0.2 μm PTFE membrane and washed with acetone to remove cyclohexanone and any unreacted monomer. The filtered product was then dried in a vacuum desiccator to remove

**Table 1**  
Reaction conditions for the synthesis of AIFA composites.

Composite	PAM-co-nAl (g)	PFDMA (g)	AIBN (g)	Cyclohexanone (mL)
AIFA-0	–	50.0	0.50	75
AIFA-10	5.0	45.0	0.45	75
AIFA-30	15.0	35.0	0.35	75
AIFA-50	25.0	25.0	0.25	75
AIFA-60	30.0	20.0	0.20	75
AIFA-70	35.0	15.0	0.15	75

residual solvent. Reaction yields between 90% and 95% were observed for each composite.

To ensure uniform distribution of the nano Al throughout the material, the composite was compounded for 3 min in a DACA Instruments benchtop twin screw extruder at 150 °C. The compounded material was then extruded through a circular die into a cylindrical clam shell mold and allowed to cool to room temperature. The final product was a gray, waxy solid with increasing metallic luster as particle content increased; the AIFA 0 composite, which does not contain any nano Al, was a white waxy solid.

#### 2.4. Characterization

Thermogravimetric analysis (TGA) was performed on a TA Instruments SDT Q600 dual TGA/DTA. Samples (5–20 mg) were placed into a tared alumina crucible with an empty alumina crucible serving as the reference. All data was collected in dynamic mode under flowing argon (100 mL/min) from room temperature up to 800 °C at a rate of 5 °C/min.

Differential Scanning Calorimetry (DSC) was performed on a TA Instruments Q1000 DSC. Samples (3–10 mg) were sealed in an aluminum pan with an empty aluminum pan serving as the reference. Each sample was subjected to a heat-cool-heat cycle to remove any stored thermal history in the material. After equilibrating at 90 °C samples were heated at 5 °C/min to a final temperature of 150 °C. Following the first heating cycle the samples were cooled from 150 °C to 90 °C at a rate of 5 °C/min and then subjected to a second heat ramp covering the same temperature range at 2 °C/min. All reported data was collected during the final heating cycle.

Transmission electron microscopy (TEM) images were acquired on a Phillips CM200 microscope with LaB<sub>6</sub> emission source at an operating voltage of 200 keV. Samples were prepared by embedding small slivers of the composites into flat molds filled with Embed 812 resin and polymerized overnight in a 60 °C oven. The blocks were then ultramicrotomed with a PowerTome XL ultramicrotome by Boeckler Instruments and a 35° Diatome diamond knife. Sections were cut at a thickness of 75 nm and a speed of 1 mm/s. Ribbons of the sections were floated onto the water trough of the diamond knife and picked up and placed onto 3 mm 400 mesh hexagonal Cu grids and allowed to air dry. Once dry, the sections were ready to be imaged in the TEM.

Pellet combustion experiments were performed by placing an 8 mm long × 4 mm diameter pellet of the respective composite onto a stainless steel wire mesh located in a vented fragmentation chamber under an air atmosphere. The pellets were initiated by a butane flame from directly below. A NAC Image Technology Memrecam® GX8 digital high speed video camera, collecting full frame, full color images at 3000 frames per second, was used to record video of the pellet combustion experiments. Images from the high speed video were subsequently analyzed using image processing software (IDL 3.1) in order to calculate intensity of reaction (light output) as a function of time.

X-ray powder diffraction (XRD) spectra were acquired on a Rigaku DMAX B RU200 spectrometer using CuK $\alpha$  radiation. Identification of the observed patterns was accomplished by comparison with the ICDD crystallographic database.

Quasi-static compression testing of 8 mm long × 4 mm diameter right circular cylinders was carried out using an MTS 820 servo hydraulic test frame, incorporating a self-aligning compression subpress (Wyoming Test Fixtures, model B 11) with precision ground steel upper and lower platens. Testing was performed according to ASTM D695 10 under displacement control at a nominal strain rate of 10<sup>-3</sup> s<sup>-1</sup>. A digital video camera and associated image correlation software (Vic Gage 2.0; Correlated Solutions, Inc.) was used to record continuous strain data from

multiple, redundant *virtual* strain gages during the testing. Simultaneous load data was obtained using a calibrated 10 kN load cell mounted on the load frame. Teflon® tape was used to lower the friction between the specimen end faces and both upper and lower loading platens, to minimize barreling. A minimum of two repeat specimens were tested for each AIFA composition.

### 3. Results and discussion

To date, PTFE has been the most prominently reported fluorinated precursor used in nano Al/polymer composite reactive systems. This is due in part to its fully fluorinated carbon backbone resulting in a fluorine density of 75% by weight, higher than any other fluorinated polymer system. Additionally, PTFE is available in both micron- and nano-scale powders that are amenable to mixing with nano Al. The main limitation of PTFE is its processability. Suspension or dispersion polymerizations are commonly used to prepare high quality PTFE [16], however these approaches require the use of both an aqueous layer and elevated temperatures, which limits the possibility of introducing nano Al to prepare nano Al/PTFE composites *in situ* since nano Al reacts with water, especially at elevated temperatures. In the present work, therefore, a solution polymerization approach was selected which would not compromise the reactivity of nano Al. Secondly, a monomer system was required that could be polymerized *in situ* with the functionalized nano Al particles and one that would yield a more processable polymer than PTFE. PFDMA was chosen since it has a highly fluorinated alkyl tail, analogous to a PTFE oligomer and contains ca. 60% fluorine by weight. PFDMA also contains a readily polymerizable methacrylic head that is amenable to free radical polymerization and is similar in structure to the PAM used to functionalize the nano Al. Furthermore, PFDMA was commercially available at a moderate cost and is compatible with many solvents making it desirable for solution polymerization.

The presence of a solvent was necessary to overcome the common viscosity and wetting issues related to the high SSA of the nano Al particles; cyclohexanone was selected to provide dissolution of the heavily fluorinated monomer, PFDMA, thereby allowing it to react with the functionalized particles during polymerization. The acting hypothesis was that the monomer coating present on the nano Al surface would co-polymerize during propagation of the growing poly(PFDMA) chains thereby providing a direct chemical linkage between the particles and the polymer matrix. The general reaction scheme is presented in Scheme 1.

The thermoplastic behavior of the poly(PFDMA) matrix allowed for successful compounding of all AIFA composites with the exception of the AIFA 70 composite. The particle content was sufficient in the AIFA 70 powder to seize the screws in the compounder. A picture of a typical processed and machined AIFA composite is displayed in Fig. 1. It is worth noting that the physical appearance of the composites increases in metallic luster as the particle content is increased.

TGA analysis was performed to confirm the particle loading of the composite materials after compounding and extrusion. A noticeable weight loss was observed slightly above 150 °C associated with degradation of the polymer matrix, likely scission and decomposition of the perfluorinated alkyl tail to yield an alkene or alcohol [19,20]. Complete degradation of the polymeric matrix was achieved by ca. 400 °C for each composite studied. The residual mass observed at 500 °C was used to determine the particle content of the composite. Figure 2 contains an overlay of the TGA curves for the respective composites along with a chart illustrating the difference in the observed particle content from the initial particle loadings used to prepare the composites. Based upon the TGA results it was clear that the *in situ* polymerization approach



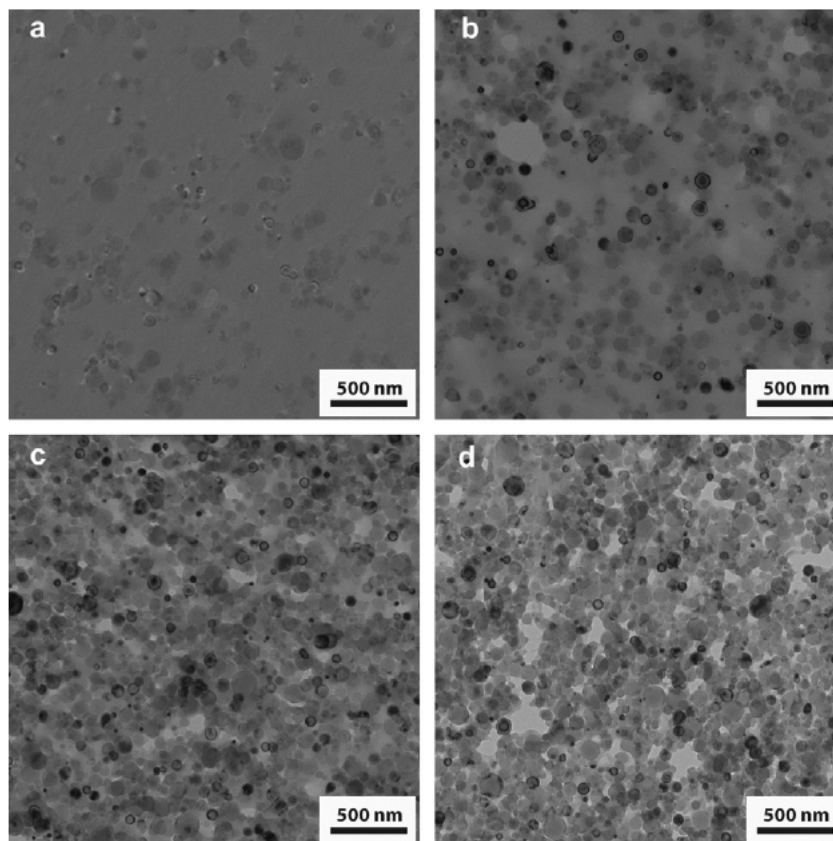


Fig. 3. TEM micrographs obtained from cross-sections of (a) AIFA-10, (b) AIFA-30, (c) AIFA-50 and (d) AIFA-60 composites.

between the two. Intimate mixing of particles with the polymer matrix is clearly evident from the micrographs. There are no visible signs of particle matrix decohesion, suggesting that the interface is continuous and that the PAM layer on the oxide surface has become integrated within the polymer matrix, as thought. Although many of the particles appear to be dispersed in a discrete non aggregated form, some aggregation still appears to be present even after compounding and extrusion. The AIFA 10 and AIFA 30 composites displayed small areas of aggregation but for the most part the particles appear to be homogeneously dispersed throughout the matrix. Moreover, there appear to be very few voids present within the sample; a proportion of the voids that are observed in Fig. 4a and b, are considered artifacts from TEM sample preparation, such as particle pullout or matrix tearing during microtomy. Aggregation was present in the consolidated AIFA 50 and AIFA

60 composites, however, it is difficult to distinguish from the matrix due to the high particle loadings. The amount of porosity in the composite materials also increased with the higher particle loadings; Fig. 3c and d show voids within aggregates that were not penetrated by monomer or polymer during polymerization or compounding and extrusion. We anticipate that these aggregates will have little effect on reactivity since they are loosely packed and maintain high surface area. Conversely, voids within the matrix will have an effect on the overall composite density, and therefore could negatively affect mechanical strength. Theoretical maximum densities (TMDs) were calculated for the 8 mm long  $\times$  4 mm dia. pellets and ranged from 99% for the neat polymer to 88% and 94% TMD for the AIFA 50 and AIFA 60 composites, respectively.

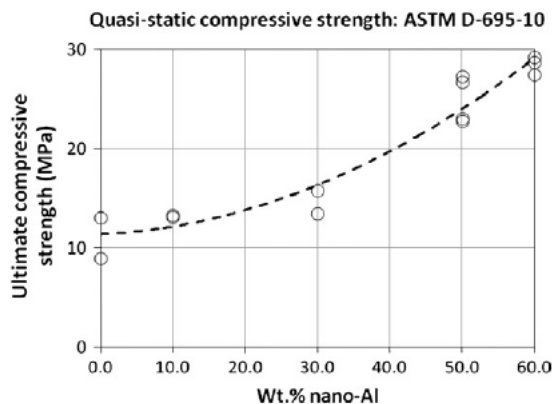


Fig. 4. Quasi-static compressive strength ( $\sigma_c^0$ ) measured as a function of nano-Al content for AIFA nanocomposites, according to ASTM D-695-10. Dashed curve is an aid for the eye.

### 3.2. Compressive strength

It was hypothesized that the compressive mechanical properties of the AIFA materials would be superior to the neat polymer due to the high particle loadings and also the direct chemical bonding between the nano Al and the polymer matrix. The neat polymer (AIFA 0) displayed a peak compressive strength of ca. 11 MPa. The addition of PAM functionalized particles into the polymer matrix resulted in an increase in compressive strength, with the highest values, ca. 25–28 MPa, obtained for the AIFA 50 and 60 composites. Figure 4 is a plot showing measured ultimate compressive stress as a function of nano Al content.

### 3.3. Combustion dynamics of AIFA composites

In addition to understanding the mechanical behavior of nano Al/fluoropolymer composites, one of the goals of the research was also to investigate the reactive properties of these materials.

Semi quantitative combustion rate experiments were performed by igniting a cylindrical pellet (8 mm long  $\times$  4 mm dia.) at each composition with a small butane flame and allowing the pellets to burn open to lab air. The combustion events were recorded with a digital high speed color video camera operating at 3000 frames per second. Figure 5 shows the evolution of the measured intensity of the video images as a function of time for the AIFA 30, AIFA 50 and AIFA 60 materials accompanied by a time sequence of full color images obtained from the combustion respective composites.

All of the composites, with the exception of AIFA 0 and AIFA 10, demonstrated a self sustaining deflagration upon ignition. Since the AIFA 0 composite did not contain any nano Al, the pellet simply melted upon heating. The AIFA 10 composite also initially melted but subsequently ignited after sustained heating. This could occur due to the loss of polymer as smoke and char until the nano Al becomes concentrated enough to sustain a reaction.

In contrast, ignition of the AIFA 30 pellet occurred immediately upon contact with the flame. A self sustaining intense

white yellow flame was observed accompanied by the production of a significant amount of smoke and black char. The char was collected and analyzed by XRD (Fig. 6) to determine the identity of the solid products. The primary component of the char was  $\text{AlF}_3$  indicating that nano Al was indeed reacting with the fluorinated polymer matrix in a similar manner to PTFE. Other products also present in the char included aluminum oxide, unreacted metallic aluminum (presumably ejected during the rapid burning), aluminum carbide ( $\text{Al}_4\text{C}_3$ ) and aluminum oxide carbide although these two products were minor compared to  $\text{AlF}_3$ .

Combustion of the AIFA 50 pellet yielded the most intense and rapid reaction, compared to the other composite compositions. The pellet ignited readily upon exposure to the butane flame producing an intense yellow orange flame that rapidly consumed the entire pellet releasing smoke and gasses which physically moved the pellet across the wire gauze as it burned. The intensity plot in Fig. 5 shows two distinct peaks, one around 500 ms and another around 1.0 s, with the deflagration process requiring around 1.3 s for

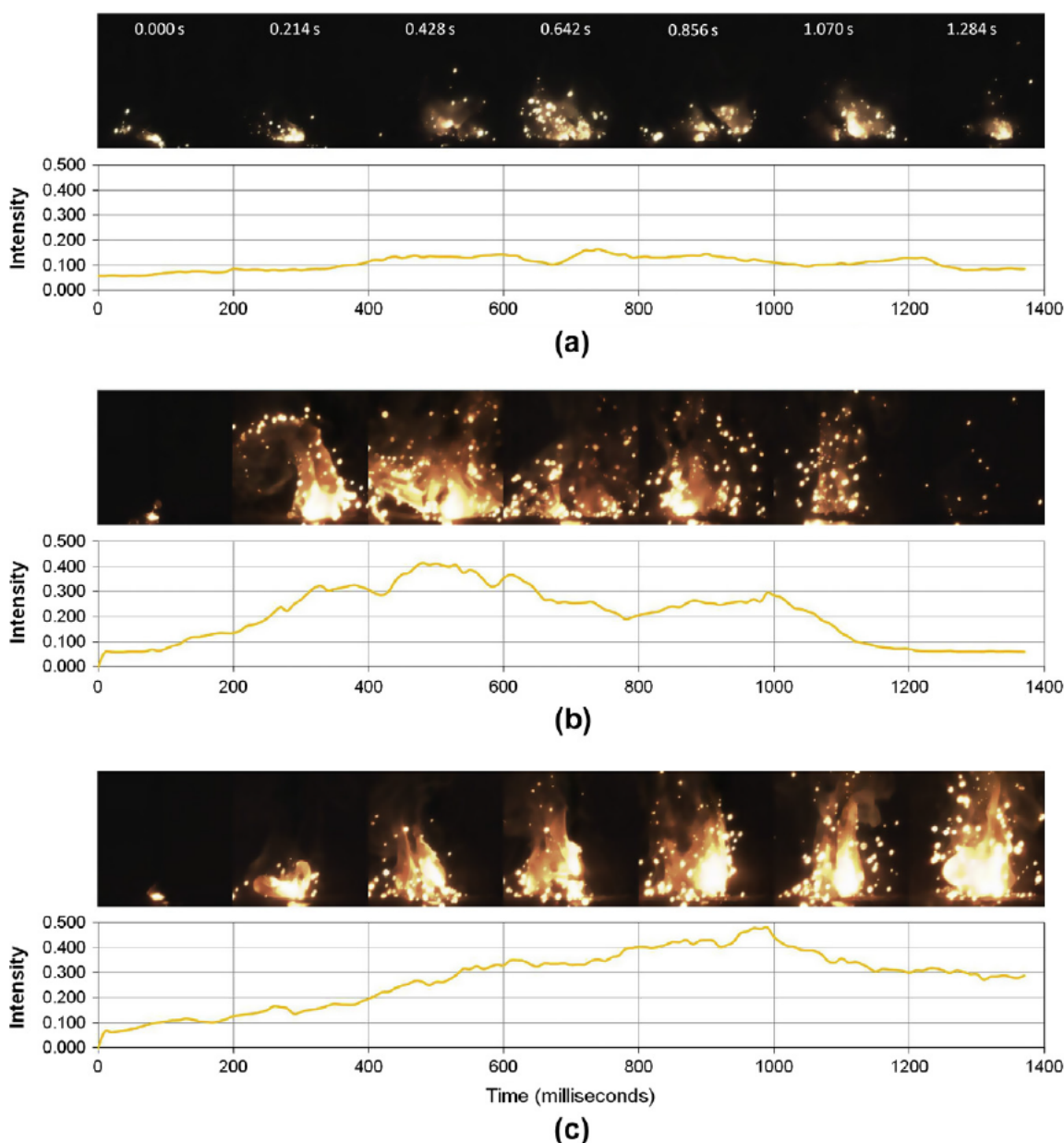


Fig. 5. Plot showing measured reaction intensity for (a) AIFA-30, (b) AIFA-50, and (c) AIFA-60 composites, based on high-speed digital video images of combusting pellets, as a function of time.

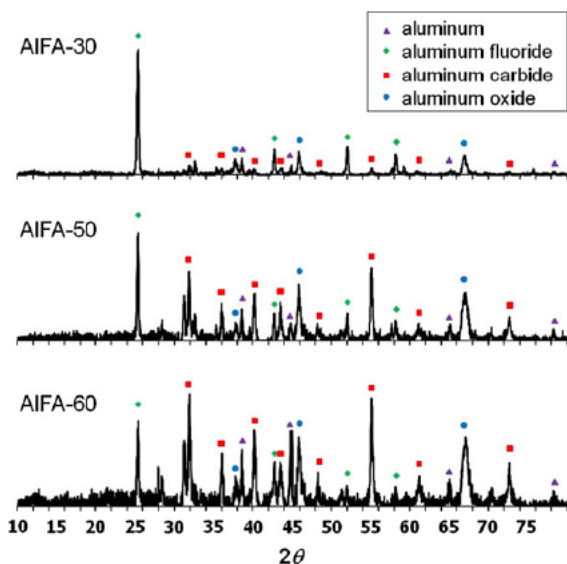
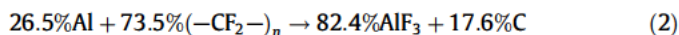


Fig. 6. XRD patterns obtained from the soot collected after completion of the combustion experiments performed on the respective AIFA composites.

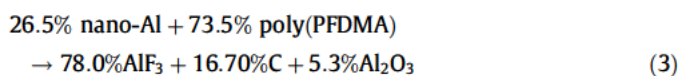
complete combustion. The char obtained as a product of the reaction was black and gray in color. XRD analysis again confirmed the presence of  $\text{AlF}_3$  as the major product, but also the  $\text{Al}_4\text{C}_3$  and aluminum oxide peaks were more prevalent than was observed for the AIFA 30 char. Residual aluminum and aluminum oxide carbide were also present but only as trace phases.

Ignition and deflagration of the AIFA 60 pellet was slower than the AIFA 50 pellet. A similar yellow orange flame was produced, which steadily grew in intensity as the reaction progressed. A total reaction time of more than 1.5 s was required to obtain complete combustion of the pellet with the most intense flames appearing *ca.* 1.0 s after ignition. The char product was primarily a dark gray color. XRD analysis confirmed  $\text{Al}_4\text{C}_3$  as the major component of the char followed by  $\text{AlF}_3$  and aluminum oxide; residual aluminum was also present as a trace phase.

The stoichiometric reaction between nano Al and PTFE resulting in  $\text{AlF}_3$  and carbon (as previously shown in Eq. (1)) requires a composition equivalent to 26.5% Al and 73.5% PTFE by weight as shown in the following equation:

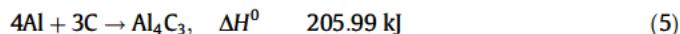
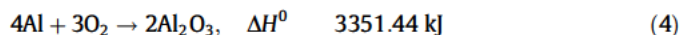


TGA oxidation studies confirmed that the nano Al used in the AIFA composites has an 80% active aluminum content due to the presence of an inert oxide shell, therefore 20% of the nano Al mass does not contribute anything to the reaction. Moreover, the poly(PFDMA) fluoropolymer contains *ca.* 60% fluorine by mass, compared to 75% for PTFE. Adjusting the stoichiometry of Eq. (3) to account for both these factors results in a stoichiometric composition for complete fluorination equivalent to 26.5% nano Al in 73.5% poly(PFDMA) fluoropolymer by weight as shown in the following equation:

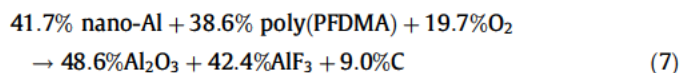
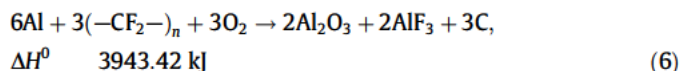


The preceding analysis provides a thermodynamic basis for  $\text{AlF}_3$  being the dominant product in the soot collected from the AIFA 30 combustion, since the AIFA 30 composition is very close to the stoichiometric condition required for complete fluorination. Moreover, AIFA 30 being slightly fuel rich leaves a small residual

amount of aluminum available to react with oxygen and/or carbon to yield the observed oxide and/or carbide products (Eqs. (4) and (5)), respectively.



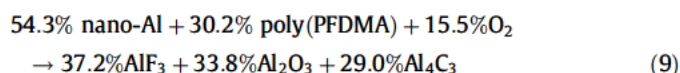
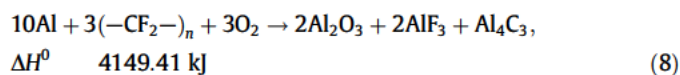
Since the open burn testing was carried out in air, it is possible that both oxidation and fluorination mechanisms can make contributions towards the overall energetic performance of the material therefore it is possible to optimize the material for both reactions by combining Eqs. (1) and (4) as shown below in Eq. (6). Once again accounting for the active aluminum and fluorine available in nano Al and poly(PFDMA), respectively, Eq. (6) can be easily translated into Eq. (7).



Examination of Eq. (7) indicates that a composition equivalent to 51.9% nano Al and 48.1% poly(PFDMA) by weight is required for optimization of both fluorination and oxidation. The AIFA 50 composition prepared for this work is very close to this stoichiometric composition and it was also the most reactive composite in combustion tests, requiring the shortest overall time to achieve complete deflagration and producing the most intense overall flame (see Fig. 6). We propose that the increased performance of the AIFA 50 composite, compared to the other AIFA composites, is due to its proximity to near stoichiometric conditions. Enough aluminum was present in the composite to support simultaneous oxidation and fluorination which produces a significant amount of heat that further accelerates diffusion between the reacting species thereby increasing the rate of reaction. Furthermore, an additional amount of energy equivalent to a maximum of 1180.50 kJ can be released by combustion of the carbon produced as a byproduct of the fluorination event.

A significant increase in the formation of  $\text{Al}_4\text{C}_3$  was observed in the AIFA 60 composite compared to the others, although some  $\text{Al}_4\text{C}_3$  was present in the AIFA 50 soot. The mechanism(s) for carbide formation are still unclear but is anticipated to occur through reaction of the aluminum with carbon, (Eq. (5)).

The carbon required to produce the carbide must come from the polymer, either in the methacrylate backbone or from carbon produced during fluorination. In the AIFA 60 composite, specifically, the composition is fuel rich with more than enough aluminum present to support fluorination and oxidation as well as carburization. Additionally, because the carbon produced from fluorination is also responsible for carbide formation then Eq. (8) is obtained which is readily translated into Eq. (9) after accounting for the active aluminum in nano Al and available fluorine in poly(PFDMA).



This corresponds to a composition of 64.3% nano Al and 35.7% poly(PFDMA) which is near the AIFA 60 composition tested in this work. Notably, the formation of an  $\text{Al}_4\text{C}_3$  phase ( $(\Delta H_f(\text{Al}_4\text{C}_3) =$

205.99 kJ/mol)[11] does not contribute significantly to the overall energetic release, since it provides only 1.88 kJ per gram of aluminum.

Deviations towards fuel lean compositions result in loss of reactivity as was observed by the lack of reaction for the AIFA 10 composite. Particle contents closer to the stoichiometric conditions for fluorination yet slightly fuel rich, such as the AIFA 30 composite, resulted in near complete reaction between the nano Al and the fluorinated matrix, with only minor phases present in the reaction products indicating both air oxidation and/or carbide formation. Since these reactions occurred in the presence of air, the prevalence of  $AlF_3$  as the dominant product of AIFA 30 combustion suggests that fluorination is kinetically favored over oxidation even though formation of the oxide is thermodynamically preferred. However, as the composition is adjusted to fuel rich conditions AIFA 50 and AIFA 60 the oxide and carbide products grow rapidly accompanied by a decrease in  $AlF_3$ . These compositions are fluorine deficient and therefore air oxidation (Eq. (4)) can compete with fluorination (Eq. (3)) and eventually becomes the dominant mechanism for aluminum consumption after the all of the fluorine has been consumed. This is supported by the intensity profiles found in Fig. 5. It is postulated that the first peak in the AIFA 50 data is due to the kinetically faster fluorination reaction (or a combination of fluorination and oxidation), and the second peak (around 1.0 s) is due solely to the oxidation of the remaining aluminum, with both reactions contributing towards the overall intensity. Moreover, if carbide is formed as a product from the reaction of nano Al with carbon produced during the initial fluorination (Eq. (5)), then this explains why the carbide phase is only present in the fuel rich mixtures since fluorination is kinetically preferred and completely consumes the aluminum under near stoichiometric conditions for fluorination (AIFA 30) leaving no aluminum available to react with the carbon.

By numerically integrating the total area under the intensity time curves, one can obtain a simple, semi quantitative measure of the extent of reaction. When this is done, it shows that the total integrated intensity scales linearly with the amount of nano Al present in the composite, Fig. 7.

This would be expected on the basis that combustion is occurring in air, i.e. with unlimited supply of oxidizer either F or O from the fluoropolymer or O from the atmosphere. Also plotted on this figure is the elapsed time from ignition to peak intensity, i.e. the deflagration time, taken from the data in Fig. 5. This gives a semi quantitative measure of the kinetics of the combustion reaction, as a function of composition. There is a minimum in the

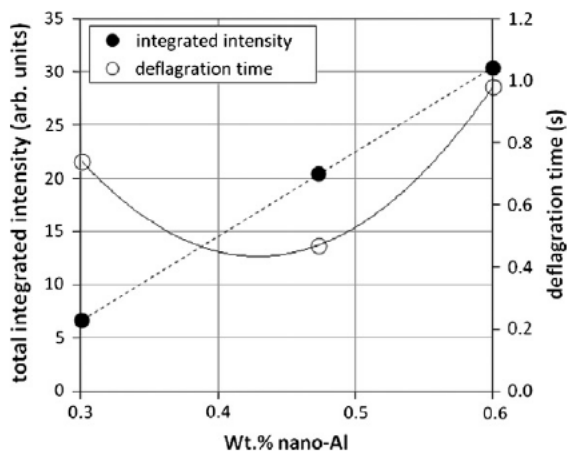


Fig. 7. Total integrated intensity (area under curves from Fig. 5; filled symbols) and deflagration time (time taken to reach peak intensity; open symbols) plotted vs. composition, for open-burn combustion testing of AIFA composites.

deflagration time that corresponds to the AIFA 50 composition, i.e. this composition has the highest overall burn rate. We postulate that this occurs because the AIFA 50 composition was nearest to the stoichiometric conditions for both fluorination and oxidation thereby providing multiple reaction pathways for consumption of the aluminum. The large plume present during combustion suggests that aluminum is being ejected from the pellet or vaporizing and is reacting in air accompanied by the combustion of the carbonaceous byproducts from the polymer and the carbon produced during fluorination. These events provide additional heat to the system thereby enhancing the overall burn rate for that composition. Additionally, the adiabatic flame temperature for oxidation of aluminum is approximately 550 °C hotter than the adiabatic flame temperature for fluorination, therefore one would expect the AIFA 50 combustion to occur faster than the pure fluorination observed in the AIFA 30 composition since the higher temperatures produced during combustion will enhance the overall rate of reaction. Similar observations have been reported for magnesium/Teflon/Viton composites [10]. By the same arguments, the AIFA 60 product takes longer to react because more aluminum is consumed through air oxidation and carbide formation due to the lack of fluorine present in the composition. These reactions are kinetically slower than fluorination and formation of the carbide, although exothermic, produces much less heat than combustion of the carbonaceous byproducts. Therefore less heat is produced to enhance the overall burn rate and a slower burn time is observed. Additionally, in order for oxygen to react with particles at the interior of the pellet the oxygen must diffuse through the surface of the pellet into the core. Since more of the pellet is comprised of aluminum more oxygen is needed to fully consume the aluminum which results in an overall slower reaction time.

#### 4. Conclusion

We have developed a new approach toward the preparation of reactive nano Al/fluoropolymer composites utilizing an *in situ* free radical solution polymerization of PFDMA in the presence of PAM functionalized nano Al. The resulting AIFA composite materials have been prepared with nano Al loadings of 10%, 30%, 50%, 60% and 70% by weight, while composites with 60 wt.% nano Al or less exhibited thermoplastic behavior and are capable of being processed through melt extrusion. Chemical integration of the nano Al particles into the fluoropolymer matrix results in a continuous phase at the particle polymer interface which was shown to enhance the mechanical performance of the material.

Open air combustion experiments performed on consolidated (extruded) pellets initiated by exposure to a butane flame resulted in a self sustaining deflagration for the AIFA 30, AIFA 50 and AIFA 60 composites. Combustion of the AIFA 30 composite primarily resulted in the formation of  $AlF_3$  as it was nearest to the stoichiometric reaction conditions for fluorination. However, since these experiments were performed open to air, combustion of the AIFA 50 composite yielded the most energetic response (minimum time for complete deflagration) as the aluminum content was high enough to allow for multiple reaction pathways including fluorination, oxidation and carburization.

#### Acknowledgments

The authors would like to acknowledge Ms. Pamela Lloyd for preparation of TEM sample specimens and Mr. W.A. Houston and Mr. J.M. Scott for technical support. Funding for this work was made available by Air Force Research Laboratory, Materials and Manufacturing Directorate, from the Nanoscience and Technology

STT Initiative in Nanoenergetics. Their support is gratefully acknowledged.

## References

- [1] E.L. Dreizin, *Prog. Energy Combust.* 35 (2009) 141–167.
- [2] A. Ingenito, C. Bruno, *J. Propul. Power* 20 (2004) 1056–1063.
- [3] G.A. Risha, S.F. Son, R.A. Yetter, V. Yang, B.C. Tappan, *Proc. Combust. Inst.* 31 (2007) 2029–2036.
- [4] A. Rai, K. Park, L. Zhou, M.R. Zachariah, *Combust. Theory Model.* 10 (2006) 843–859.
- [5] C.E. Aumann, G.L. Skofronick, J.A. Martin, *J. Vac. Sci. Technol., B* 13 (1995) 1178–1183.
- [6] P. Brousseau, C.J. Anderson, *Propellants, Explos., Pyrotech.* 27 (2002) 300–306.
- [7] C.D. Yarrington, S.F. Son, T.J. Foley, *J. Propul. Power* 26 (2010) 734–743.
- [8] K.W. Watson, M.L. Pantoya, V.I. Levitas, *Combust. Flame* 155 (2008) 619–634.
- [9] M.L. Pantoya, S.W. Dean, *Thermochim. Acta* 493 (2009) 109–110.
- [10] E.-C. Koch, *Propellants, Explos., Pyrotech.* 27 (2002) 340–351.
- [11] D.R. Lide (Ed.), *CRC Handbook of Chemistry and Physics*, 77th ed., CRC Press, Boca Raton, FL, 1996.
- [12] I. Glassman, R.A. Yetter, *Combustion*, fourth ed., Academic Press, Burlington, MA, 2008.
- [13] R.J. Jouet, A.D. Warren, D.M. Rosenburg, V.J. Bellitto, K. Park, M.R. Zachariah, *Chem. Mater.* 17 (2005) 2987–2996.
- [14] D. Stamatis, X. Zhu, M. Schoenitz, E.L. Dreizin, P. Redner, *Powder Technol.* 208 (2011) 637–642.
- [15] J.J. Granier, M.L. Pantoya, *Combust. Flame* 138 (2004) 373–383.
- [16] J. Scheirs, *Fluoropolymers – Technology, Markets and Trends*, Smithers Rapra Technology, Shawbury, UK, 2001.
- [17] C.A. Crouse, C.J. Pierce, J.E. Spowart, *ACS Appl. Mater. Interface* 2 (2010) 2560–2569.
- [18] The average molecular weight of PAM was calculated to be 238.14 g/mol based on the reported 25% diester content and a molecular weight of 178.61 g/mol for the mono-ester.
- [19] V.V. Zuev, F. Bertini, G. Audisio, *Polym. Degrad. Stab.* 91 (2006) 512–516.
- [20] S.C. Moldoveanu, *Analytical Pyrolysis of Synthetic Organic Polymers*, Elsevier, Amsterdam, The Netherlands, 2005.